Journal of Agricultural Sciences
(Tarim Bilimleri Dergisi)

J Agr Sci-Tarim Bili
e-ISSN: 2148-9297
jas.ankara.edu.tr

JAS

Possibilities of Using Regional Index-Flood Method with Annual Maximum and Partial Duration Series: A Case Study of Susurluk River Basin, Turkey

Ayşe Doğanülker[a], Alper Serdar Anli[a*], Havva Eylem Polat[a]

[a]*Ankara University Agricultural Faculty Agricultural Structures and Irrigation Department, 06110, Diskapi, Ankara, TÜRKIYE*

ARTICLE INFO
Research Article
Corresponding Author: Alper Serdar Anli, E-mail: asanli@agri.ankara.edu.tr
Received: 01 July 2024 / Revised: 26 August 2024 / Accepted: 29 August 2024 / Online: 14 January 2025

Cite this article
Doğanülker A, Anli A S, Polat H E (2025). Flood Method and Annual Maximum and Partial Duration Series: A Case Study of Susurluk River Basin, Turkey. *Journal of Agricultural Sciences (Tarim Bilimleri Dergisi),* 31(1):161-181. DOI: 10.15832/ankutbd.1508286

ABSTRACT
Among the natural disasters experienced in Turkey, floods, which cause the most loss of life and property after the earthquake, have increased their impact and frequency of occurrence over time, as well as unplanned urbanization caused by the increasing population, uncontrolled construction in stream beds, and changing climate. Therefore, it is important to accurately predict the magnitude and frequency of floods. This study investigated the possibilities of using the regional index-flood method and annual maximum series (AMS) and partial duration series (PDS) in the Susurluk River basin. Annual maximum flood series provided homogeneity in the Susurluk basin as a single region, and the Generalized Logistic (GLO) distribution fits the AMS. PDS was extracted according to the threshold levels determined using the variance-mean ratio and frequency factors. The PDS's most appropriate frequency factors (k) were determined according to the Poisson distribution, which makes the variance-mean ratio equal. k=3.5 was determined for only two stations. k=4 was suitable for seven stations, and k=5 was suitable for thirteen stations. The average number of peaks over the threshold level (λ`) varies between 1.26 and 5.31. Since PDS is not homogeneous in a single region, cluster analysis divided the basin into three regions. After homogeneity was achieved, Pearson Type 3 (PE3) and Generalized Pareto (GPA) distributions were suitable with the PDS. The study concluded that instead of annual maximum flood series, partial duration flood series can be used in many stations in the short and medium term but can be used in fewer stations in the long-term estimations. Since Regions I and II are relatively lower and flatter areas than Region III, it was observed that the flows started to accumulate at the stations in these regions, and larger floods were predicted. Region III is close to the basin upstream, and smaller floods were predicted at the stations in this region. Since partial duration flood estimations are lower than annual maximum flood ones, they can provide advantages to engineering projects with lower costs. In addition, PDS can be useful in regionalizing floods, which are very common due to the data extraction process.

Keywords: Peaks-over-threshold, frequency factor, L-moments, regional frequency analysis, design flood, Susurluk basin

1. Introduction

Hydrology studies the cycle, distribution, properties, and environmental effects of water on the atmosphere, surface, and underground. As the need for water increases over time, it has become an increasingly important branch of science. Therefore, water distribution, protection, and control have become vital. Flood is a situation where the amount of water in stream beds suddenly increases due to the excess rainfall in the basin, overflows from the stream bed, and damages the living beings, soil, and property around it. The acceleration of the hydrological cycle due to global climate change and designs according to incorrect flow rates have increased the frequency of floods today (Doğanülker 2022).

Many precautions have been taken against floods: Preventing settlements in areas with stream beds, reducing damage to the design of water structures, and controlling floods. Strong forecasts of floods are important to be able to take these precautions. It is impossible to have precise information about when and how much a future flood will occur. For this reason, floods can be estimated using appropriate statistical methods using data obtained from flow observation stations established at certain points on the stream (Anlı et al. 2007). One of these methods is frequency analysis (how much and at what intervals a flood will occur in the future), and the data obtained from the selected region for analysis must cover a period long enough to make the event sufficient. Flood frequency is an analysis performed by finding the most compatible probability distribution with the peak flow values occurring in a region. The expected result of this frequency analysis is that the estimated flood magnitude is close to the desired recurrence period (Fill & Steiner 2003). Two types of series are frequently used in flood frequency analysis: Annual maximum & partial-duration flood series. The series created from the maximum flows occurring once in a water year is called the annual maximum flood series. The series extracted with data higher than a specified threshold value instead of the maximum value taken yearly is called a partial-duration series (Seçkin 2009). Flood frequency analysis can be applied with two different techniques: at-site and regional. Since at-site flood frequency analysis is obtained using hydrological data at a single flow station,

reliable results cannot be obtained when similar situations are calculated from different stations. In basins where no measurements or insufficient measurements have been made; the regional flood frequency analysis method is used to estimate flood flows. Previous studies on at-site and regional frequency analysis of annual maximum and partial flood series have been attempted to be summarized chronologically.

Cunnane (1979) investigated the fit of the Poisson distribution to partial duration series using data from 20 stations in 20 basins in Great Britain. Ben-Zvi (1991) tested the fit of negative Binomial and Poisson distributions to partial duration flood series using data from 8 hydrometric stations in temporary rivers in Israel. A range of threshold levels were considered at each station. Positive results were obtained at the 5% significance level in 30 out of 53 tests for the Poisson distribution and 22 out of 28 for the negative Binomial distribution. Rasmussen & Rosbjerg (1991) stated that dividing the year into a certain number of seasons is important to correctly represent the data above the threshold value determined in the partial duration series. However, they stated that the seasonal models extracted are unsuitable for predictions because they require many parameters. Their study estimated seasonal and non-seasonal return periods by applying the Exponential and Poisson distributions to those exceeding the threshold value. As a result, they stated that the most suitable estimates were mostly obtained in the non-seasonal model. Rosbjerg et al. (1992) stated in their studies that the assumption that the data above the threshold value determined in the partial duration series is suitable for the Exponential distribution is suitable for the Generalized Pareto distribution. Wilks (1993) performed frequency analysis using annual maximum and partial duration data taken from stations in the USA. He analysed the performance of 8 three-parameter probability distributions and stated that the beta-k distribution most accurately represented the rightmost tail of the annual maximum data. He also observed that the Beta-P distribution best represented the partial duration series. The two-parameter Gumbel distribution gave below-prediction probabilities in annual maximum and partial duration data at high rainfall amounts. Madsen et al. (1997a) used the Generalized Pareto distribution for the partial duration series and the Generalized Extreme Values distribution for the annual maximum series in the study. Madsen et al. (1997b) stated that in the regional analysis where partial duration and annual maximum series were compared, partial duration series gave the best results with Generalized Pareto distribution and annual maximum series with Generalized Extreme Values distribution. The accuracy of the partial duration series Generalized Pareto, and annual maximum series Generalized Extreme Values regional index-flood models were compared using Monte Carlo simulation, and it was revealed that the partial duration series data of the defined regions were more homogeneous than the annual maximum series. Lang et al. (1999) emphasized that annual maximum flood continues to be the most well-known approach in frequency analysis. They stated that the difficulties associated with using an alternative, the peaks over threshold approach, are the selection of thresholds and flood peak protection criteria. They argued that the literature on the peaks over threshold model is limited and inconsistent. Anlı (2009), in his regional frequency analysis study focusing on precipitation in Ankara using the L-moment method, used annual maximum and partial duration series and stated that generally more accurate results were obtained with high probabilities in the partial duration data set and that the partial duration data set could be used as an alternative to the annual maximum data set in at-site regional precipitation estimates. Rahman et al. (2013), in a regional flood frequency analysis study for semiarid and arid regions of Australia, found that the Generalized Pareto distribution was preferable to the Exponential distribution for the application of partial duration flood data in arid regions and determined that arid regions exhibited a much steeper flood frequency growth curve than humid regions. Bezak et al. (2014) stated that the peaks over the threshold data set provided more accurate results than the annual maximum data set for data obtained from a measurement station in Slovenia. They stated that the Binomial distribution did not provide a noticeable improvement over the Poisson distribution in modelling the number of annual exceedances of the threshold. Pham et al. (2014) examined the performance of the partial duration series and aimed to determine the regional λ (The average number of peaks over the threshold) value. According to the results obtained, they observed that the Generalized Pareto distribution best explains the partial duration series in the region and stated that they achieved the best partial duration series/Generalized Pareto performance when the λ value was equal to 5. Guru (2016) observed that the Generalized Pareto distribution in India best describes the partial duration series in the region and also observed that the λ' value in the most accurate partial duration series/Generalized Pareto relationship was found at 2, 2.5, and 3. Karim et al. (2017) showed in their study that frequency estimates based on partial series were better than those based on annual series for small and medium-sized floods, and both methods gave similar results for large floods. In their study, Zadeh et al. (2019) stated that the technique of regionalizing peaks over threshold series generally improved flood estimation compared to regionalizing annual maximum series. Ahmad et al. (2019) observed that Generalized Extreme Values with L-moment parameter estimation methods in partial duration and annual maximum series were the most suitable statistical distributions for partial duration series. Generalized Logistic was the most suitable statistical distribution for the annual maximum series. They also concluded in the study that the partial duration series performed better than the annual maximum series in estimating amounts for the most suitable probability distributions. Swetapadma & Ojha (2021) applied maximum entropy theory in partial duration series modelling of flood frequency analysis to find the appropriate threshold level and related distribution patterns in New Zealand. They concluded that it can be used as a good method for threshold determination in partial duration series of flood frequency studies.

Other important similar studies on partial duration series in recent years are as follows: Askhar & Ba (2017) applied the four-parameter Kappa distribution to partial duration flood series, Durocher et al. (2019) studied non-stationary frequency analysis on partial duration flood series with the help of the regional index-flood method, Agilan et al. (2020) used the Generalized Pareto distribution as non-stationary frequency analysis on partial duration series, Van Campenhout et al. (2020) emphasized that hourly data should be investigated in partial duration series, not daily, Kiran & Srinavas (2021) applied regional frequency analysis to both annual maximum and partial duration flood series and obtained various regression models, Pan & Rahman (2021)

investigated the differences in annual maximum and partial duration flood series estimates with the help of basin physiographic features, Guru (2022) mentioned the difficulty in finding the average number of peaks over threshold (λ') and tried to estimate with various methods, Pan et al. (2022) investigated the superiority of partial duration flood series over annual maximum series, Yue et al. (2022) examined partial duration rainfall series with non-stationary frequency analysis, Amorim & Villarini (2024) performed trend analysis with parametric and non-parametric methods in partial duration series with Generalized Pareto distribution.

There are few studies in Turkey where partial duration flood series and regional analysis are applied. There is also no study in the Susurluk basin, where floods cause damage. This study aims to investigate the possibilities of using partial duration flood series on a regional and at-site basis as an alternative to annual instantaneous maximum flood data in the Susurluk River basin using the regional index-flood approach and to assist flood risk management.

2. Material and Methods

2.1. Study area and data

The Susurluk basin, a key area of more than 2 million hectares in the west of Turkey, is a significant player in water resources management. Situated between 39°-40° north latitudes and 27°-30° east longitudes, the basin's total rainfall area is 22 399 km^2, with an average annual flow of 5.43 km^3. In the south of the Marmara Region, the basin is home to numerous large and small rivers that flow continuously or for short periods, making it a crucial resource for the region's water needs (Gürler et al. 2024). Susurluk Basin covers some of the rapidly growing provinces such as Bursa, Kütahya, Balıkesir, Çanakkale, Bilecik, Manisa, and İzmir. Floods are even more dangerous for those living in these cities, where the population increases daily. Especially in the Osmangazi district of Bursa province, located in the north-east of the basin, flood events have occurred from time to time, and various precautions and evacuation plans have been made in the reports prepared by the General Directorate of Water Management in this region for environmental impact assessment, human health and protection against floods. Other areas of the basin are affected by floods at medium and low risk (SYGM 2022). Since cities are located in areas with high flood risk, the risk of damage resulting from floods and possible major accidents is also high. This research used annual maximum and partial duration flood series among daily flow rates for flood frequency analysis and for determining flood risk. Susurluk Basin was chosen for regional flood frequency analysis due to its location. Daily streamflow discharges obtained from 22 streamflow observation stations were used in the study. Some characteristics of the streamflow observation stations operated by the General Directorate of State Hydraulic Works (DSI) and the previously closed Electrical Works Survey and Development Administration (EIE) in the basin are given in Table 1. The observation periods of the stations are from the date of commencement of operation to the last evaluation year. Streamflow rates were naturalized by the institutions from which they were obtained (DSI and EIE). The study consists of a master's thesis and started in 2021. Therefore, the streamflow data from the stations used are until 2016 and 2017. The observation period of the stations varies between 25-68 years. Streamflow data was obtained continuously for the specified years. The data set of the stations operated by DSI is shorter, while the data set of the stations operated by EIE is longer. While DSI stations are generally operated to determine the capacity of water storage structures, EIE stations are operated for both this purpose and research purposes. In addition, the streamflow data of both institutions are uninterrupted in the Susurluk basin. Many small and large streams in the basin flow continuously or for short periods. While the flows of these streams contain very little water, especially in the summer and early autumn months due to agricultural water use, they reach quite high levels in the winter and spring with the amount of melting snow. The locations of the streamflow observation stations in the Susurluk basin, where the daily flow rates used as material in the research were obtained, are shared in Figure 1.

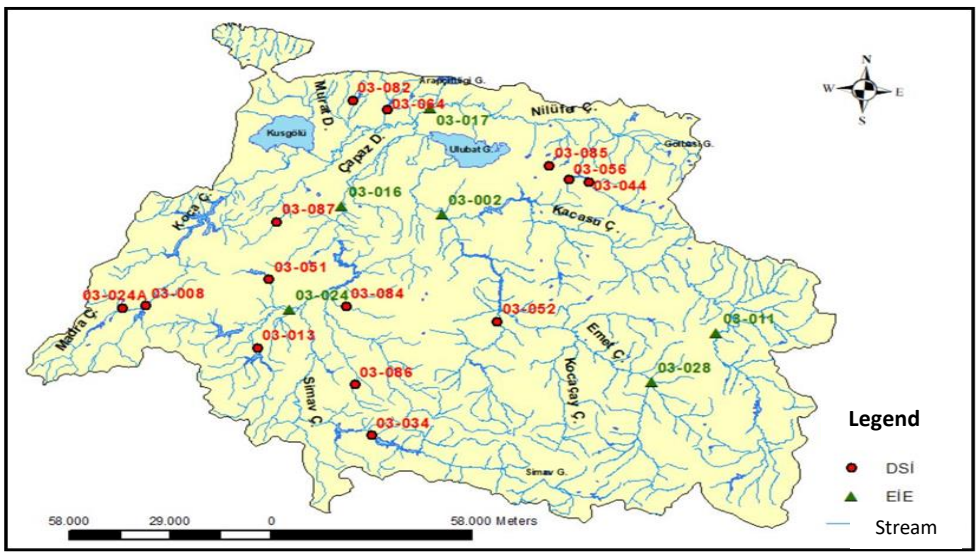

Figure 1- The location of the streamflow observation stations in the Susurluk Basin

Table 1- Characteristics of the streamflow observation stations in the Susurluk Basin

No	*Station code*	*Station name*	*Longitude–Latitude (°)*				*Precipitation area (km²)*	*Elevation (m)*	*Observation period*	*Sample size*
1	D03A008	Kahve	27.54	East	39.61	North	741	190	1969–2016	48
2	D03A013	İkizcetepeler	27.92	East	39.50	North	467	128	1972–2017	46
3	D03A024	Ayaklı	27.36	East	39.52	North	115	250	1967–2016	50
4	D03A034	Osmanlar Köp.	28.32	East	39.25	North	1266	277	1979–2017	39
5	D03A044	S.Saygı Brj. Gir.	29.00	East	40.08	North	377	341	1987–2017	31
6	D03A051	Değirmenboğazı	27.95	East	39.71	North	84	192	1981–2017	37
7	D03A052	Sinderler	28.72	East	39.62	North	965	294	1983–2017	35
8	D03A056	Sultaniye	28.94	East	40.09	North	50	368	1989–2017	29
9	D03A064	Gölecik	28.28	East	39.61	North	111	27	1993–2017	25
10	D03A082	Keçiler	28.18	East	40.30	North	21	65	1990–2017	28
11	D03A084	Eyüpbükü	28.23	East	39.65	North	241	945	1986–2017	32
12	D03A085	İnegazi	28.87	East	40.13	North	15	306	1989–2017	29
13	D03A086	Adalı	28.26	East	39.39	North	66	375	1987–2017	31
14	D03A087	Yeşilova	27.96	East	39.90	North	141	250	1991–2017	27
15	D03A096	Okçular	28.30	East	39.40	North	35	405	1991–2017	27
16	E03A002	Döllük	28.51	East	39.62	North	9617	40	1950–2017	68
17	E03A011	Küçükilet	29.86	East	39.12	North	1642	795	1955–2017	63
18	E03A016	Yahyaköy	28.17	East	39.98	North	6376	32	1954–2017	64
19	E03A017	Akçasusurluk	28.40	East	40.26	North	20	2	1957–2017	61
20	E03A024	Balıklı	28.02	East	39.63	North	244	94	1958–2017	60
21	E03A028	Dereli	29.25	East	39.46	North	1165	557	1969–2017	49
22	E03A031	Dağgüney	29.06	East	39.92	North	3493	365	1992–2017	26

2.2. Methods

2.2.1. Selection of annual maximum flood series

The annual maximum flood series used in the research are meticulously selected, considering the largest values from the data obtained from the time series of a hydrological event within a year. This careful selection process ensures the reliability of our findings.

2.2.2. Extraction of partial duration flood series

A partial duration flood series to be used in the research is a series consisting of independent events (m) that all exceed the selected threshold value (x_0) at a station and are subtracted from the observation period (n). Adamowski et al. (1998) stated that non-annual exceedance series were selected. In extracting the partial duration series, it is essential to choose the threshold value, specify the peak flow rates that exceed the predicted threshold value, and determine parameter estimates and probability distributions for modelling the size of these peaks. A series larger than the estimated threshold value and more ($m > n$) values than the observation year is selected. The selection of the threshold value when creating a non-annual exceedance series is obtained by the variance-mean ratio (σ^2/μ) method. The purpose of this method is explained by the fact that the mean and variance of the Poisson distribution are equal. Therefore, if the distribution of peak numbers fits with the Poisson distribution, the ratio of the variance (σ^2) to the mean (μ) of the peak numbers occurring each year (exceeding the threshold value) during the observation period is expected to be equal to or close to one (Adamowski 2000). In recent years, partial duration series models derived from this method have been used by some researchers (Pan et al. 2022; Yue et al. 2022; Amorim & Villarini 2023).

When selecting the threshold value, it will be assumed that the number of values exceeding the threshold value determined as a trial from the beginning for each year fits with the Poisson distribution, which is a discrete distribution given in Equation 1 (Cunnane 1979);

$$P(z\ pik > x_0) = P_z = e^{-\lambda}\ \lambda^z / z! \quad (1)$$

Where: P_z= probability of the number of peaks over a threshold in each year, z= the number of peaks over a threshold value in each year, x_0 = threshold value, λ = mean of the distribution.

When determining non-annual exceedance series, first, various values at a station are tried until a condition is obtained where the variance-mean ratios (σ^2/μ) are one or very close to one throughout the observation period. Then, flood discharges are selected among the observations according to this condition. As a result, it is reached that the average number (λ') of the peaks exceeding the experimentally selected threshold value at the stations throughout the observation period is greater than one. A flood data lower than the largest flood data chosen each year in the annual maximum series may also cause floods, and the results obtained in a design based on annual maximum flood discharges may not be sufficient. For this reason, the partial duration series (peaks-over-threshold level) method is used. One of the most important points in the partial duration series is the threshold level (x_0) selection. For this purpose, the frequency factor equation 2 given by Rosbjerg & Madsen (1992) was used in the study.

$$x_0 = E\{Q\} + kS\{Q\} \qquad k \geq 1 \tag{2}$$

Where: $E\{Q\}$= average daily flow rates (m^3/s), $S\{Q\}$= standard deviation of daily flow rates (m^3/s), k= frequency factor, x_0= threshold level (m^3/s)

2.2.3. Parameter estimation methods

Given that it's not feasible to determine all aspects of a random variable, it becomes the responsibility of researchers, statisticians, and students in probability and statistics to estimate the parameters of the probability distribution function using the sample of the variable. The shape, scale, skewness, kurtosis, and symmetry in the probability distribution function are all tied to these parameters. They are crucial in defining the statistical characteristic of a random variable in a given distribution (Önöz 1994). This research focused on the sequence models' probability-weighted moments, L-moments, and L-moment ratios, as outlined by Kjeldsen et al. (2002).

2.2.4. Probability-weighted moments

This method, developed by Greenwood et al. (1979), was later investigated by Hosking (1986). As a result of the research, it was observed that central statistics have similar properties to moments. It has been concluded that while the estimates of the mentioned moments are unbiased, especially for small samples, they are sensitive to values at data points that deviate significantly from the trend of the existing data. Modifications and distortions in inappropriate data significantly affect the statistical parameters calculated for small data. In addition, this technique shows a much lower effect from sampling changes than other moments since they are a linear data function. This feature provides superiority over other methods (Önöz 1994). Probability weighted moments are;

$$M_{p,r,s} = E\,[X^p\{F(X)\}^r\{1 - F(X)\}^s] \tag{3}$$

In Equation 3, X represents the statistical data, and $F(X)$ represents the cumulative distribution function of X. Probability-weighted moments, $\alpha_r = M_{1,0,r}$, and $\beta_r = M_{1,r,0}$ are used for the minimum probability of occurrence (exceedance) and the maximum probability of occurrence (non-exceedance), respectively. Probability-weighted moments of α_r and β_r are used as the basic method in parameter estimation of probability distributions. The probability-weighted moment of β_r is used in the case of ascending order of data, and a weighted moment of α_r is used in the case of descending order. In this research, the weighted moment of β_r is used and given in Equation 4 (Hosking 1986);

$$\beta_r = E[X\{F(X)\}^r] \qquad r = 0, 1, 2, \ldots \tag{4}$$

In Equation 4, the probability-weighted moment β_r is equal to the product of the powers (r) of the cumulative distribution function $F(X)$ of the X data. Here, the $F(X)$ function represents the probability function where X is weighted differently for different r values. For the value r= 0, the β_0 value is equal to the population mean ($E(X)$) (Haktanır & Bozduman 1995).

However, since it is difficult to specify the scale and shape of a probability distribution with probability-weighted moments directly, some linear combinations of these moments were created using the ordinal statistics explained below (Haktanır 1991; Seçkin & Topcu 2016).

2.2.5. L-moments method

Greenwood et al. (1979) express a linear function of the probability-weighted moments. This technique was developed through Hosking (1990). The observation statistics of the method, widely used in solving various problems such as regionalization and distribution, can be easily calculated without the need to square and cube the data. Although this technique is less sensitive to long-term data than normal product moments, it is generally similar to known moments. Therefore, the L-moment function of a data X is expressed as probability-weighted moments. From the observations here, X (n:j) is an *unbiased sample estimate* of the probability weight moments obtained by Greenwood et al. (1979), which is expressed in the following equation;

$$b_r = j^{-1} \sum_{n=1}^{j} \frac{(n-1)(\mathrm{n}-2)\ldots(\mathrm{n}-\mathrm{r})}{(j-1)(j-2)\ldots(j-r)} x_{n:j} \quad (5)$$

First four b_r values (r= 0, 1, 2, 3) and probability weighted moments (b_0, b_1, b_2, and b_3) are found, then L-moment statistics for any distribution,

$$\ell_1 = b_0, \quad (6)$$

$$\ell_2 = 2b_1 - b_0, \quad (7)$$

$$\ell_3 = 6b_2 - 6b_1 + b_0, \quad (8)$$

$$\ell_4 = 20b_3 - 30b_2 + 12b_1 - b_0 \quad (9)$$

The first L-moment, ℓ_1 is a measure of central tendency and is equivalent to the mean of the distribution. The measure of distribution is ℓ_2. The estimated dimensionless L-moment ratio;

$$t = \frac{\ell_2}{\ell_1} (L - coefficient\ of\ variation, L - Cv) \quad (10)$$

$$t_3 = \frac{\ell_3}{\ell_2} (L - skewness, L - Cs) \quad (11)$$

$$t_4 = \frac{\ell_4}{\ell_2} (L - kurtosis, L - Ck) \quad (12)$$

The above-mentioned b_1 and b_2, L-coefficient of variation, t and t_3 and t_4, in other words, L-moment ratios, are the most useful measures that briefly express probability distributions. L-moments of different distributions can be easily represented with the L-moment ratio diagram. In two-parameter distributions, only two values expressed as measurement and position parameters are distributed in any way. L-kurtosis and L-skewness values are equal and are indicated in the diagram with only one dot. In a three-parameter distribution, the parameters included are scale, location, and shape. In these three-parameter distributions, different points are determined with varying shape parameters to define them with a line (Hosking & Wallis 1997, Topcu & Seçkin 2016).

2.2.6. Index-flood method

In the index-flood method, the hypothesis is that the recurrence distributions of the data at all stations are the same, except for a scale factor. In the process, stations are methodically and rigorously divided into homogeneous regions by various analyses, ensuring the reliability of the results. It is extremely effective in combining summary statistics of separate data sets. The index-flood approach (Dalrymple, 1960) and its variants (Basu & Srinavas 2016, Stedinger 1983, Sveinsson et al. 2003, Öney & Anlı 2023) are widely used for regional frequency analysis. If there is a station i with N data in a basin with n_i stations and it is assumed that these data are defined in the form Q_{ij}, j= 1,..., n_i; Q_i (F); The assumption expressed as a quantile function of the non-exceedance probability of station's data i (F);

$$Q_i(F) = \mu_i\, q(F), \qquad i = 1,\ldots, N. \quad (13)$$

In this equation, μ_i; the index-flood value represents the average probability distribution at the station. This value represents the rainfall and surface flow characteristics in each basin and. it defines the regional growth curve of the non-exceedance probability of the q (F) value (F), which is equal for all stations. By multiplying the q (F) value obtained in the regional frequency analysis with the average of the desired station (F), the Q_i (F) value of the hydrological variable at the station to which it belongs is reached for the return period. Common regional frequency distribution function applied to dimensionless data;

$$q(F) = Q_{ij}/\mu_i \quad (14)$$

2.3. Stages of regional frequency analysis

Hosking & Wallis (1993) define the stages used in regional frequency analysis as follows: Preliminary statistical analysis of the data (Discordancy measure), determination of hydrologically homogeneous regions (Heterogeneity measure), determination of the best regional probability distribution (Goodness-of-fit measure), and development of the regional probable flood discharges (Regional L-moment algorithm).

2.3.1. Discordancy measure

The Discordancy measure (D_i) plays a crucial role in ensuring the accuracy of the data in regional frequency analysis. By reviewing the collected values, this measure enables the elimination of major inaccuracies and the detection of incompatibilities, thereby ensuring the compatibility of the stations separated as homogeneous regions.

$$D_i = \frac{1}{3} N(u_i - \bar{u})^T K^{-1}(u_i - \bar{u}) \tag{15}$$

According to the equation, u_i represents the vector of L-moment ratios at a particular station, $\bar{u}$ represents the mean of the vector, and K represents the covariance matrix of this vector. The fact that the D_i is higher than the critical tabular value, which varies depending on the number of stations in the region, leads to the conclusion that the station is completely discordant (Hosking & Wallis 1997).

2.3.2. Heterogeneity measure

When determining the homogeneity of a region based on the discordancy measure, it's crucial to calculate the heterogeneity of the groups at the stations. This involves comparing the L-moment variations of regions that are likely to be particularly homogeneous at stations. To calculate the heterogeneity measure, we first assume the basins to be homogeneous. We then compute the mean and standard deviations of the selected dispersion measure by simulating the values of a station in a homogeneous region in similar observations. The H statistic is then used to compare the dispersion measures obtained.

$$H = \frac{(V_{obs} - \mu_v)}{\sigma_v} \tag{16}$$

$$V_{obs} = \left\{ \frac{\sum_{i=1}^{N} n_{i\left(\tau_2^i - \tau_2^R\right)^2}}{\sum_{i=1}^{N} n_i} \right\}^{\frac{1}{2}} \tag{17}$$

While the weighted standard deviation calculated from regional data by looking at various L-moment ratios is expressed with the V_{obs} statistic, μ_v and σ_v represent the average and standard deviation values of the number of simulations of this statistic. N is the number of stations; n_i is the sample size of any station, τ_2^i is the sample L-coefficient of variation of any station, and τ_2^R is the regional sample L-coefficient of variation. The difference between the L-moment ratios at the stations and the regional L-moment ratios calculates the V_{obs} statistic. In Equation 17, only V_{obs} related to the H_1 statistic is given. Equations H_2 and H_3 are calculated similarly. In this research, the four-parameter Kappa distribution was used. Compared to two- and three-parameter distributions, this distribution is stronger since it expresses more than one distribution in the frequency analysis of hydrological events. For μ_v and σ_v values to provide more accurate results, the number of simulations will be considered 500 for a region. According to all these statements, the basin: If $H < 1$, it is acceptably homogeneous; if $1 < H < 2$, it may be heterogeneous; and if $H > 2$, it is not homogeneous. An attempt is made to achieve homogeneity by dividing a un homogeneous region into sub-regions.

2.3.3. Goodness-of-fit measure

Only a probability distribution shows the best fit for the data obtained from homogeneous stations. A Z^{DIST} statistic measure has been recommended for the goodness-of-fit criterion related to the L-kurtosis ratio and a random probability distribution. The equation of this method is as follows;

$$Z^{DIST} = \frac{(\tau_4^{DIST} - t_4^R + B_4)}{\sigma_4} \tag{18}$$

$$B_4 = N_{sim}^{-1} \sum_{m=1}^{N_{sim}} \left(t_4^{(m)} - t_4^R \right) \tag{19}$$

$$\sigma_4 = \left[\left(N_{sim} - 1 \right)^{-1} \left\{ \sum_{m=1}^{Nsim} \left(t_4^{(m)} - t_4^R \right)^2 - N_{sim} B_4^2 \right\} \right]^{1/2} \tag{20}$$

In this equation, t_4^R is defined as the L-kurtosis ratio of the regional mean value of the sample, while B_4 is the bias value and σ_4 is its standard deviation. In Equations 19 and 20, N_{sim} is defined as the number of simulations made using the Kappa four-parameter distribution, and m is defined as the number of areas simulated. In this study, Generalized Extreme Values (GEVs), Generalized Logistic (GLO), Generalized Pareto (GPA), Pearson Type 3 (PE3), and Generalized normal (GNO) distributions were used. Their cumulative distribution F (x) and quantile x (F) functions are given in Table 2. If the absolute $Z^{DIST} \leq 1.64$ in

any distribution, this distribution is considered suitable for regional distribution. This value corresponds to a 90% confidence level. However, among the distributions examined, the absolute Z^{DIST} value closest to zero is determined as the best-fit distribution.

Table 2- Cumulative distribution *F* (*x*) and quantile *x* (*F*) functions of the regional frequency distributions used in the study

Distribution	*Code*	*F (x), x (F)*
Generalized Extreme Values	GEVs	$F = \exp[-\{1-k(x-\xi)/\alpha\}^{1/k}]$ $x = \xi + \alpha\{1-(-\log F)^k\}/k$
Generalized Logistic	GLO	$F = 1/[1+\{1-k(x-\xi)/\alpha\}^{1/k}]$ $x = \xi + \alpha[1-\{(1-F)/F\}^k]/k$
Generalized Normal	GNO	$F = \Phi[-k^{-1}\log\{1-k(x-\xi)/\alpha\}]$ $x(F)$ not precisely defined
Generalized Pareto	GPA	$F = 1-\{1-k(x-\xi)/\alpha\}^{1/k}$ $x = \xi + \alpha\{1-(1-F)^k\}/k$
Pearson type 3	PE3	$F = G\left((x-\mu+2\sigma/\gamma)/\lvert\frac{1}{2}\sigma\gamma\rvert, 4/\gamma^2\right), \quad \gamma > 0$ $F = 1-G\left(-(x-\mu+2\sigma/\gamma)/\lvert\frac{1}{2}\sigma\gamma\rvert, 4/\gamma^2\right), \quad \gamma < 0$ $x(F)$ not precisely defined
Kappa	KAP	$F = [1-h\{1-k(x-\xi)/\alpha\}^{1/k}]^{1/h}$ $x = \xi + \alpha[1-\{(1-F)^h/h\}^k]/k$
Wakeby	WAK	$F(x)$ not precisely defined $x = \xi + \frac{\alpha}{\beta}\{1-(1-F)^{\beta}\} - \frac{\gamma}{\delta}\{1-(1-F)^{-\delta}\}$

$G(x,\alpha) = \{\Gamma(\alpha)\}^{-1}\int_0^x t^{\alpha-1}e^{-t}dt$ missing gamma integral.

$\Phi(x) = (2\pi)^{-1/2}\int_{-\infty}^{x}\exp(-t^2/2)dt$ standard normal cumulative distribution function.

2.3.4. Regional L-moment algorithm

The study used a regional algorithm that combines at-site statistics of L-moments with index-flood and weighted average methods. In the regional L-moment algorithm stage, a probability distribution adapted to the homogeneous region value is selected. The means of the probability distributions at all stations, accepted as index-flood data, are reliable and provide a confident basis for the data at the stations obtained by the sample mean of the at-site value.

The sample mean of a station with n_i data in an area with N stations is stated as ℓ_1^i. Sample L-moment ratios are obtained as $t^{(i)}, t_3^{(i)}, t_4^{(i)}$. The average L-moment ratio of each station during the observation period is calculated in the form t^R, t_3^R, t_4^R;

$$t^R = \frac{\sum_{i=1}^{N} n_i t^{(i)}}{\sum_{i=1}^{N} n_i} \tag{21}$$

Taking the regional average $\ell_1^R = 1$

$$t_r^R = \frac{\sum_{i=1}^{N} n_i t_r^{(i)}}{\sum_{i=1}^{N} n_i} \qquad r = 3, 4,\ldots \tag{22}$$

and from here the regional population (λ_i and τ_i) and sample L-moment ratios (ℓ_1^R, t_1^R) are equalized;

$$\lambda_1 = \ell_1^R$$
$$\tau = t^R \quad (23)$$
$$\tau_3 = t_3^R$$

Flood quantiles at the desired probability and return period along with dimensionless regional growth curves;

$$\hat{Q}_i(F) = \ell_1^i q(F; \ell_1^R, t^R, t_3^R, t_4^R) \quad (24)$$

FORTRAN 77 source codes written through Hosking (2005) were used in all these calculations, and (l-moments, version 3.04) routines were used. The routines collected under a basic program were arranged and executed.

3. Results and Discussion

3.1. Regional frequency analysis with annual maximum flood series

The annual maximum flood series were selected using the annual instantaneous maximum flood data in the DSI flow observation yearbook of the stations in the research. As a result of the discordancy measure (D_i) test determined using this data set, no discordant stations were detected in the annual maximum series within the 22 stations; in other words, it was concluded that the basin was homogeneous in a single region case (Table 3). The discordancy measure test consists of a test that determines the harmony between stations' L-moment ratios. In this study, among the annual maximum flood series obtained from 22 stations, no discordancy was detected between the L-moment ratios of any station flood data, based on the $D_{critical\ value}$ given in Hosking & Wallis (1997) and varying according to the number of stations in the region (All $D_i < D_{critical\ value}$: 3.00). This shows that the annual maximum flood data in the Susurluk basin does not have any discordant conditions in a single region. After this stage, whether the basin was homogeneous or not was tested.

On the other hand, when the L-moment ratios are examined in Table 3, the annual maximum flood data is skewed to the right at all stations. L-kurtosis ratios show that the flood data is flat at some stations and sharp at others. Accordingly, the annual maximum flood data is not normally distributed (Ahmad et al. 2019).

After no discordant station was achieved, the heterogeneity measure (H) was calculated. The heterogeneity measure compares the inter-site variations in sample L-moments for the group of sites with what would be expected of a homogeneous region. While H_1 and H_2 measures provided homogeneity (< 1.00) in the calculations, the H_3 measure showed possible heterogeneity case (> 1.00). However, since H_1 and H_2 measures provide the homogeneity conditions, the basin is accepted as homogeneous (Table 4). When Table 4 is examined, although the H_3 test value shows that the region is probably heterogeneous, it is clear that the region is homogeneous since the H_1 and H_2 test values are very close to zero. Negative heterogeneity measures (H_1 and H_2) indicate that the spread between stations is quite low and homogeneity is strong. It has been stated that regional frequency analysis is more effective than at-site frequency analysis, even if the basin considered in many regionalization studies is somewhat heterogeneous (Hosking & Wallis 1997; Anlı 2009; Van Campenhout et al. 2020; Kiran & Srinavas 2021; Pan & Rahman 2021).

Susurluk basin was obtained as a homogeneous region according to the annual maximum flood series as a single region, generalized logistic (GLO), generalized extreme values (GEVs), generalized normal (GNO), generalized Pareto (GPA) and Pearson type 3 (PE3) distributions were selected as candidates to estimate frequency distributions suitable for annual instantaneous flood discharges. The generalized logistic (GLO) distribution emerged as the only suitable distribution for annual maximum flood discharges among these distributions (Ahmad et al. 2019). Other frequency distributions still need to be able to describe the annual maximum flood data. L-kurtosis and Z^{DIST} (Goodness-of-fit measure) values found according to the candidate distributions are shown in Table 5. Regional L-kurtosis ratios of frequency distributions show that annual maximum floods are flat. Design flood discharges estimated by the regional L-moment algorithm obtained according to various recurrence probabilities and return periods are shown in Table 6. According to Table 6, the average (Q_2) design flood flow discharge is approximately 128 m^3/s. The spillway design discharge of small water storage structures ($Q_{50\text{-}100}$) is approximately 422-520 m^3/s, the diversion channel discharge (Q_{25}) is approximately 341 m^3/s, and the main irrigation channel project (Q_{10}) is approximately 254 m^3/s. It can be approximately 80-88 m^3/s for secondary and tertiary channel projects ($Q_{1.25\text{-}1.33}$) and 21-60 m^3/s for city drainage networks ($Q_{1.01\text{-}1.11}$). Since the basin is homogeneous according to the annual maximum flood data, design flood flow values can be considered for the entire Susurluk basin, but in the following section, at-site frequency analysis was carried out for each station separately with the L-moment parameter method.

Table 3- Mean, L-moment ratios, and discordancy measures (D_i) calculated for annual maximum flood series

N	*Station code*	*Mean*	*L-coefficient of variation*	*L-skewness*	*L-kurtosis*	D_i
1	D03A008	378.32	0.2543	0.0945	0.1316	0.91
2	D03A013	69.36	0.6664	0.5676	0.3566	1.40
3	D03A024	132.53	0.3590	0.3663	0.2389	0.32
4	D03A034	166.35	0.3821	0.2519	0.1684	0.47
5	D03A044	84.21	0.5180	0.4428	0.2348	1.19
6	D03A051	52.97	0.4480	0.3853	0.3967	1.49
7	D03A052	165.84	0.4002	0.4371	0.3609	0.77
8	D03A056	13.13	0.4936	0.4926	0.2923	1.01
9	D03A064	56.59	0.3263	0.2473	0.2002	0.26
10	D03A082	27.58	0.3619	0.3076	0.3098	0.66
11	D03A084	57.82	0.3064	0.1160	0.0454	2.17
12	D03A085	4.79	0.3793	0.3840	0.3660	1.15
13	D03A086	11.78	0.2459	0.1683	0.1785	0.79
14	D03A087	62.70	0.3110	0.1778	0.1524	0.56
15	D03A096	10.50	0.3156	0.2827	0.2343	0.39
16	E03A002	435.79	0.3304	0.2711	0.2159	2.16
17	E03A011	48.16	0.4295	0.3469	0.2488	0.19
18	E03A016	518.34	0.2653	0.1392	0.2493	2.21
19	E03A017	410.88	0.2550	0.0999	0.1681	0.98
20	E03A024	221.36	0.2314	0.0040	0.1552	1.56
21	E03A028	90.60	0.5138	0.4848	0.3694	0.77
22	E03A031	83.42	0.3230	0.2251	0.2716	0.58
	Weighted mean	148.44	0.3697	0.2852	0.2427	

Table 4- Heterogeneity measure results for annual maximum flood series

Heterogeneity measure	*Value*
H_1	-0.0777
H_2	-0.0553
H_3	1.1551*

*Possibly heterogeneous

Table 5- Regional L-kurtosis and goodness-of-fit (Z^{DIST}) results for annual maximum flood series

Regional frequency distribution	*L-kurtosis*	Z^{DIST}
GLO	0.234	-1.49*
GEVs	0.206	-2.72
GNO	0.187	-3.56
PE3	0.153	-5.02
GPA	0.131	-5.97

*Suitable distribution

Table 6- Regional flood discharges estimated index-flood method according to various recurrence probabilities and return periods according to the generalized logistic frequency distribution for annual maximum flood series (m^3/s)

***P* %**	1	5	10	20	25	50	80	90	96	98	99
T_{year}	1.01	1.05	1.11	1.25	1.33	2	5	10	25	50	100
***Q* (*F*)**	20.99	44.54	59.43	79.62	87.98	127.8	197.44	253.53	341.22	422.35	520.18

3.2. Regional frequency analysis with partial duration flood series

While partial duration flood series were extracted using the variance-mean ratio method, the mean and standard deviation of daily flow discharges measured at flow observation stations were calculated. According to the values obtained from daily flow discharges at flow observation stations, the standard deviation of daily flow discharges at all stations was greater than the means. If the standard deviation of a data is greater than its mean, it indicates that the data is heterogeneously distributed. While determining the threshold level, a threshold value was determined for each station using various frequency factor values (k=1, 2, 3, 3.5, 4.0, 4.5, and 5). When the frequency factor was used with a value greater than 5, the selected threshold level values were quite high. Hence, the number of above-threshold flood data was lower than the annual maximum flood series, and the $m > n$ condition was not provided. Since the threshold levels remained very low at k=1 and k=2, this caused much more flood data to be selected and made the study difficult as the number of samples increased greatly.

To determine the most suitable frequency factors according to stations, discrete probability distributions, Poisson, Binomial, and negative Binomial, were applied, and the Kolmogorov-Smirnov goodness-of-fit test determined suitable distributions. The aim is to ensure that the ratio of the variance of the peak numbers that exceed a certain threshold level and occur each year to their average is equal to or very close to one. As a result of the analyses, a frequency factor was determined for each station, prioritizing compliance with the Poisson distribution (Cunnane 1979; Ben-Zvi 1991; Rasmussen & Rosbjerg 1991; Bezak et al. 2014), Table 7 shows the Kolmogorov-Smirnov test results obtained from trial-and-error to choose the most appropriate discrete distribution for the frequency factors used in selecting the threshold level. After determining the threshold level for each station, the flood discharges above the threshold level were determined, and partial duration flood series were extracted. The Binomial distribution applied for partial duration flood discharges above the threshold levels obtained by the frequency factors providing the variance-mean ratio did not fit any data set in Table 7. The negative Binomial distribution fits very few data sets (Bezak et al. 2014). However, since the priority was the Poisson distribution, the analysis progressed according to this distribution's goodness of fit test values. The frequency factor (k=3) was not determined for any station, while k=3.5 was determined for only two stations. k=4 was suitable for seven stations, and k=5 was suitable for thirteen stations. On the other hand, the k=5 value chosen at station E03A017, the total m value was smaller than the annual maximum flood series ($m < n$), so a frequency factor of k=4.5 was considered. Since high-frequency factors are considered in most of the stations, the number of partial-duration flood discharges obtained is at a reasonable level. Threshold levels are determined using daily flow discharges, the number of partial duration flood data extracted according to these threshold levels, the average number of peaks over the threshold level, their means, L-moment ratios, and discordancy measures (D_i) are given in Table 8. Figure 2 also compares the sample size of the annual maximum and partial-duration flood series.

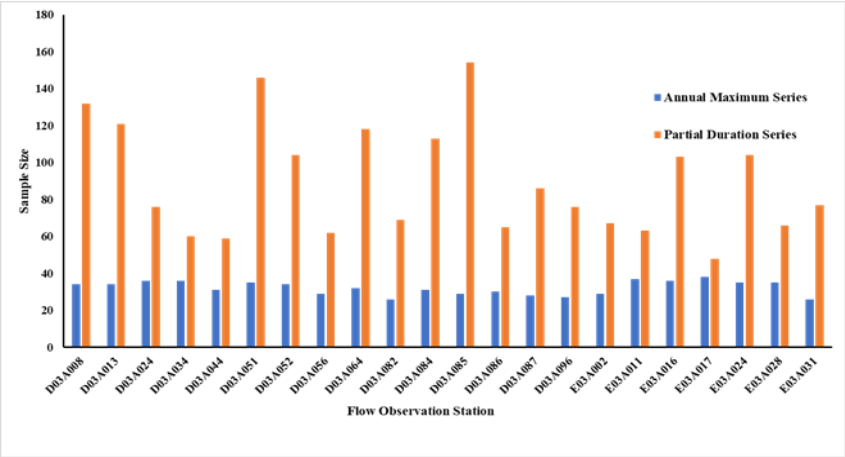

Figure 2- Sample size comparison of annual maximum and partial duration flood series.

The lowest threshold level was determined at station D03A085 with 1.64 m^3/s, and the highest threshold level was determined at station E03A017 with 612.6 m^3/s. E03A017 station is at the basin outlet point, and its elevation is 2 m. When the sample size of partial-duration flood extracted is examined, the average number of peaks over the threshold level (λ`) varies between 1.26 and 5.31 (Pham et al. 2014). Of course, the lowest and highest threshold levels are inversely proportional to ($\lambda$`) values. Therefore, the lowest flood data (m= 48) was extracted at station E03A017, and the highest flood data (m= 154) was extracted at station D03A085. The mentioned situation can also be seen in Figure 2. L-moment ratios show that the partial duration flood data is mostly right-skewed, flattened, and not normally distributed. When all partial duration series obtained from 22 stations in the Susurluk basin were subjected to regional analysis as a single region, station E03A002 was found to be discordant with the test value 4.52. L-moment ratio diagrams are given in Figure 3. In Figure 3, the discordant station E03A002 is circled. Since this station is important due to its observation period and location, it was not removed from the data set, and no outliers were sought. Therefore, according to Ward's Linkage Squared Euclidean Distance method, the basin was divided into sub-regions with cluster analysis.

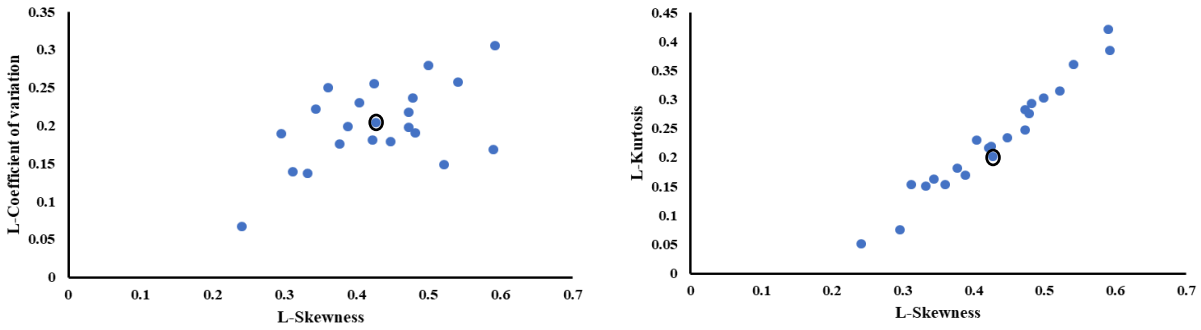

Figure 3- L-moment ratio diagrams with L-skewness versus L-coefficient of variation and L-kurtosis for E03A002 discordancy situation

The basin is subjectively divided into three sub-regions according to the cluster dendrogram in Figure 4. Sub-basin physiographic-hydrological characteristics used in the vectors of cluster analysis: elevation, latitude, longitude, precipitation area, maximum and minimum elevation of watersheds, watershed slope, and long-term average flow values. There were five stations in Region I, six in Region II, and eleven in Region III. While Regions I and II had lower-elevation flat stations, Region III had stations in the mountainous parts of the basin. This situation facilitated partial duration flood series for examining the basin in two geographical ways: flat and mountainous (Pan & Rahman 2021). Figure 5 shows the location of the stations in the homogeneous regions obtained according to the partial-duration flood series.

On the other hand, L-moment ratios show that the data is mostly right-skewed, flattened, and not normally distributed. The basin was subjected to regional analysis in its current form, and no discordant station was found in the three regions (Table 9). By performing cluster analysis, small sub-regions with fewer stations were obtained instead of having stations in a single region as a large cluster. Therefore, the harmony between fewer stations was investigated. Thus, no discordant station was detected in all three regions obtained. After no discordant station was achieved for each of the three regions, the heterogeneity measure values (H) were calculated and given in Table 10. While H_1 and H_2 measures provided homogeneity (< 1.00), the H_3 measure showed definitely heterogeneity case (> 2.00) for Region I. However, since H_1 and H_2 measures provide the homogeneity conditions, Region I is accepted as homogeneous. All heterogeneity measure results for Regions II and III revealed that these regions were acceptably homogeneous. Since all remaining H values, except the H_3 value in the first region, are very close to zero, it is clear that all three regions are satisfactorily homogeneous.

Three-parameter GLO, GEVs, GNO, PE3, and GPA probability distributions were applied to three separate homogeneous regions according to partial duration flood series, and the regional L-kurtosis and goodness-of-fit test (Z^{DIST}) results for estimating frequency distributions are given in Table 11. In Table 11, PE3 and GPA distributions in the first and second regions fit the data as expected. In contrast, GPA and GNO distributions in the third region fit the partial duration flood series. Rosbjerg (1992), Madsen et al. (1997a), Madsen et al. (1997b), Rahman et al. (2013), Guru (2016), Agilan et al. (2020), Amorim & Villarini (2024) also fitted the GPA distribution to the partial duration series. Unlike these studies, the partial-duration flood series were also fitted to the PE3 distribution in our current study. Regional L-kurtosis ratios show that the data is almost flat. Design flood discharges estimated by regional L-moment algorithm obtained according to various recurrence probabilities and relevant return periods are shown in Table 12. In Figure 6, the regional design flood discharges of annual maximum and partial duration flood series are compared to various return periods.

Table 7- Kolmogorov-Smirnov test results according to certain frequency factors and discrete probability distributions in the selection of partial duration flood series for all stations

N	*Station code*	*Discrete Probability Distribution, K-S*											
		Poisson				*Binomial*				*Negative Binomial*			
		Frequency Factor (k)											
		3.0	*3.5*	*4.0*	*5.0*	*3.0*	*3.5*	*4.0*	*5.0*	*3.0*	*3.5*	*4.0*	*5.0*
1	D03A008	0.458	0.347	0.333*	0.355	NF	NF	NF	NF	NF	NF	NF	NF
2	D03A013	0.537	0.518	0.485*	0.554	NF	NF	NF	NF	NF	NF	NF	NF
3	D03A024	0.302	0.312	0.270	0.226*	NF	NF	NF	NF	0.204	0.194	0.219	NF
4	D03A034	0.455	0.405	0.423	0.294*	NF	NF	NF	NF	NF	NF	NF	NF
5	D03A044	0.436	0.432	0.394*	0.409	NF	NF	NF	NF	NF	NF	NF	NF
6	D03A051	0.256	0.232	0.204*	0.214	NF	NF	NF	NF	0.291	0.360	0.397	0.353
7	D03A052	0.337	0.298	0.205*	0.241	NF	NF	NF	NF	0.251	0.263	0.322	NF
8	D03A056	0.354	0.310	0.334	0.278*	NF	NF	NF	NF	NF	NF	NF	NF
9	D03A064	0.251	0.166*	0.188	0.253	NF	NF	NF	NF	0.373	0.393	0.440	0.283
10	D03A082	0.316	0.282	0.246	0.206*	NF	NF	NF	NF	NF	NF	NF	NF
11	D03A084	0.287	0.251	0.176*	0.188	NF	NF	NF	NF	0.283	0.243	0.332	0.327
12	D03A085	0.396	0.386*	0.475	0.420	NF	NF	NF	NF	NF	NF	NF	NF
13	D03A086	0.336	0.307	0.293	0.240*	NF	NF	NF	NF	0.313	0.252	NF	0.387
14	D03A087	0.308	0.296	0.350	0.291*	NF	NF	NF	NF	0.172	NF	NF	NF
15	D03A096	0.362	0.307	0.278	0.259*	NF	NF	NF	NF	0.238	NF	0.260	NF
16	E03A002	0.399	0.361	0.331	0.250*	NF	NF	NF	NF	NF	NF	NF	NF
17	E03A011	0.548	0.565	0.614	0.546*	NF	NF	NF	NF	NF	NF	NF	NF
18	E03A016	0.350	0.342	0.329	0.328*	NF	NF	NF	NF	NF	NF	NF	NF
19	E03A017	0.637	0.701	0.770	0.612**	NF	NF	NF	NF	NF	NF	NF	NF
20	E03A024	0.313	0.293	0.273	0.232*	NF	NF	NF	NF	NF	NF	NF	NF
21	E03A028	0.464	0.504	0.395	0.318*	NF	NF	NF	NF	NF	NF	NF	NF
22	E03A031	0.458	0.347	0.333*	0.355	NF	NF	NF	NF	NF	NF	NF	NF

K-S: Kolmogorov-Smirnov test value; *Best-fit discrete distribution and relevant frequency factor; **While determining the threshold level with a frequency factor of k = 5.0, since the number of peaks exceeding the threshold level was obtained less than the observation period, a frequency factor of k = 4.5 was considered; NF: Non-fit discrete probability distribution

According to Table 12a, the average (Q_2) design flood flow discharge is approximately 62.15 m^3/s. The spillway design discharge of small water storage structures ($Q_{50\text{-}100}$) is approximately 170-195 m^3/s, the diversion channel discharge (Q_{25}) is

approximately 146 m^3/s, and the main irrigation channel project (Q_{10}) is approximately 114 m^3/s. It can be approximately 50-51 m^3/s for secondary and tertiary channel projects ($Q_{1.25\text{-}1.33}$) and 45-46 m^3/s for urban drainage networks ($Q_{1.01\text{-}1.11}$) for the first region. For the second region, the average (Q_2) design flood discharge was estimated to be approximately 210.65 m^3/s. Spillway design flood discharge of small dam structures ($Q_{50\text{-}100}$) is approximately 442-495 m^3/s, and diversion channel flood discharge (Q_{25}) is approximately 390 m^3/s. The main irrigation canal project (Q_{10}) is approximately 322 m^3/s. It can be evaluated as approximately 184-187 m^3/s in secondary and tertiary channel projects ($Q_{1.25\text{-}1.33}$) and approximately 176-179 m^3/s in urban drainage networks ($Q_{1.01\text{-}1.11}$) (Table 12b). When the third region design flood rates were examined, the Q_2 design flood flow rate was estimated to be approximately 36 m^3/s. The spillway design flood discharge of pond structures ($Q_{50\text{-}100}$) is about 112-139 m^3/s, and the diversion channel flood discharge (Q_{25}) is about 89 m^3/s. The main irrigation canal project (Q_{10}) is approximately 65 m^3/s; in secondary and tertiary canal projects ($Q_{1.25\text{-}1.33}$), it is approximately 30 m^3/s, and in urban drainage networks ($Q_{1.01\text{-}1.11}$), it is approximately 27 m^3/s (Table 12c). Among the three regions, the lowest design flood discharges were obtained in the third region. This is because the third region is in the mountainous regions on the upstream side of the basin, and the streamflow discharges have not yet been collected. The second region with the highest flood values is near the basin outlet point (downstream) (Pan & Rahman 2021). Annual maximum flood discharges (AMS) obtained from a single region according to various return periods with the regional L-moment algorithm were compared with partial duration flood discharges (PDS-I, PDS-II, and PDS-III) determined separately for three regions. Among them, the highest design flood discharges were obtained in PDS-II during the remaining return periods, except for Q_{100}, the upper tail of the distribution. The highest flood discharge in Q_{100} was obtained in AMS. AMS, PDS-I, and PDS-III are estimated close to each other in the lower tail of the distribution at $Q_{1.01}$. In $Q_{1.05}$, AMS and PDS-I were almost the same, while PDS-III was slightly lower.

Table 8- Threshold levels determined by using daily flow rates (x_0), the number of partial duration flood data extracted according to these threshold levels (m), the average number of peaks over the threshold level (λ`), their means, L-moment ratios and discordancy measures (D_i)

N	*Station code*	*Sample size (n)*	*Threshold level (x_0)*	*Partial duration sample size (m)*	*λ` (m/n)*	*Mean*	*L-coefficient of variation*	*L-skewness*	*L-kurtosis*	*D_i*
1	D03A008	34	69.483	132	3.88	122.77	0.2214	0.3434	0.1622	0.56
2	D03A013	34	26.204	121	3.56	45.14	0.2369	0.4784	0.2760	0.14
3	D03A024	36	30.160	76	2.11	49.53	0.2174	0.4721	0.2819	0.15
4	D03A034	36	75.680	60	1.67	112.81	0.1759	0.3763	0.1821	0.12
5	D03A044	31	31.580	59	1.90	57.47	0.3057	0.5924	0.3844	1.21
6	D03A051	35	5.640	146	4.17	10.12	0.2553	0.4251	0.2198	0.30
7	D03A052	34	55.950	104	3.06	93.45	0.2570	0.5413	0.3601	1.04
8	D03A056	29	5.060	62	2.14	6.74	0.1689	0.5906	0.4215	2.02
9	D03A064	32	8.920	118	3.69	16.43	0.2498	0.3602	0.1540	0.61
10	D03A082	26	7.080	69	2.65	10.28	0.1905	0.4820	0.2938	0.29
11	D03A084	31	13.790	113	3.65	24.18	0.2297	0.4046	0.2299	0.60
12	D03A085	29	1.640	154	5.31	2.36	0.1810	0.4219	0.2167	0.36
13	D03A086	30	5.380	65	2.17	7.88	0.1790	0.4479	0.2336	0.59
14	D03A087	28	14.910	86	3.07	23.11	0.1989	0.3877	0.1691	0.91
15	D03A096	27	2.940	76	2.81	4.05	0.1389	0.3119	0.1530	2.17
16	E03A002	29	329.630	67	2.31	499.24	0.2044	0.4274	0.2020	4.52**
17	E03A011	37	38.770	63	1.70	73.70	0.2797	0.4994	0.3023	0.24
18	E03A016	36	350.600	103	2.86	473.07	0.1371	0.3321	0.1512	1.83
19	E03A017	38	612.60	48	1.26	707.25	0.0669	0.2408	0.0513	1.63
20	E03A024	35	93.490	104	2.97	149.11	0.1898	0.2961	0.0757	1.37
21	E03A028	35	37.490	66	1.89	54.38	0.1973	0.4728	0.2481	0.93
22	E03A031	26	63.570	77	2.96	85.04	0.1486	0.5213	0.3148	0.42

λ`: average number of peaks over the threshold level; ** *discordant station*

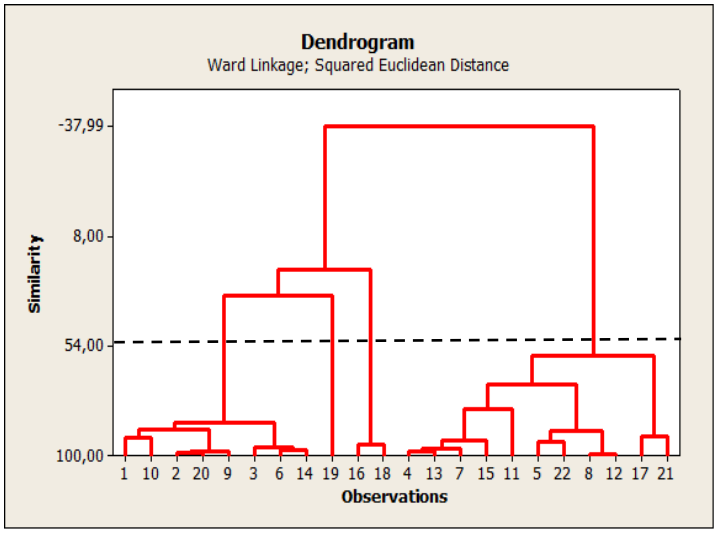

Figure 4- Dendrogram of cluster analysis

Table 9- Means, L-moment ratios, and discordancy measures (D_i) of partial duration flood series according to sub-regions

N	*Station code*	*Sample size*	*Mean*	*L-coefficient of variation*	*L-skewness*	*L-kurtosis*	D_i
			Region I				
1	D03A008	132	122.77	0.2214	0.3434	0.1622	1.27
2	D03A013	121	45.14	0.2369	0.4784	0.2760	0.90
9	D03A064	118	16.43	0.2498	0.3602	0.1540	1.13
10	D03A082	69	10.28	0.1905	0.4482	0.2938	0.59
20	E03A024	104	149.11	0.1898	0.2961	0.0757	1.10
			Region II				
3	D03A024	76	49.53	0.2174	0.4721	0.2819	1.08
6	D03A051	146	10.12	0.2553	0.4251	0.2198	0.38
14	D03A087	86	23.11	0.1989	0.3877	0.1691	0.95
16	E03A002	67	499.24	0.2044	0.4274	0.2020	1.62
18	E03A016	103	473.07	0.1371	0.3321	0.1512	0.82
19	E03A017	48	707.25	0.0669	0.2408	0.0513	1.15
			Region III				
4	D03A034	60	112.81	0.1756	0.3763	0.1821	1.25
5	D03A044	59	57.47	0.3057	0.5924	0.3844	0.76
7	D03A052	104	93.45	0.2570	0.5413	0.3601	1.23
8	D03A056	62	6.74	0.1689	0.5906	0.4215	2.31
11	D03A084	113	24.18	0.2297	0.4046	0.2299	0.44
12	D03A085	154	2.36	0.1810	0.4219	0.2167	0.71
13	D03A086	65	7.88	0.1790	0.4479	0.2236	0.90
15	D03A087	76	4.05	0.1389	0.3119	0.1530	1.84
17	E03A011	63	73.70	0.2797	0.4994	0.3023	0.47
21	E03A028	66	54.38	0.1973	0.4728	0.2481	0.87
22	E03A031	77	85.04	0.1486	0.5213	0.3148	0.20

Table 10- Heterogeneity measure (*H*) results for partial duration flood series for each region

Heterogeneity measure	*Region I*	*Region II*	*Region III*
H_1	-0.1432	-0.0740	-0.1414
H_2	-0.1347	-0.0497	-0.1453
H_3	2.6896**	0.7506	0.7787

**: Definitely heterogeneous

Table 11- Regional L-kurtosis and goodness-of-fit test (Z^{DIST}) results for estimating regional frequency distributions

Regional frequency distribution									
GLO		***GEVs***		***GNO***		***PE3***		***GPA***	
Region I									
L-kurtosis	Z^{DIST}	**L-kurtosis**	Z^{DIST}	**L-kurtosis**	Z^{DIST}	**L-kurtosis**	Z^{DIST}	**L-kurtosis**	Z^{DIST}
0.290	4.79	0.272	3.93	0.240	2.45	0.187	-0.07**	0.210	1.02*
Region II									
0.294	4.52	0.276	3.72	0.244	2.29	0.189	-0.14**	0.215	1.00*
Region III									
0.346	2.64	0.334	2.16	0.294	0.54*	0.226	-2.22	0.282	0.04**

*: Suitable distribution; **: Best-fit distribution

Table 12- Flood discharges estimated index-flood method for homogeneous regions according to various recurrence probabilities and return periods according to suitable distributions for partial duration flood series (m^3/s)

Region I (a)											
PE3 distribution											
***P* %**	1	5	10	20	25	50	80	90	96	98	99
T_{year}	1.01	1.05	1.11	1.25	1.33	2	5	10	25	50	100
***Q* (*F*)**	45.46	45.99	46.93	49.46	51.01	62.15	91.00	114.21	145.77	170.04	194.55
GPA distribution											
***P* %**	1	5	10	20	25	50	80	90	96	98	99
T_{year}	1.01	1.05	1.11	1.25	1.33	2	5	10	25	50	100
***Q* (*F*)**	44.18	45.25	46.67	49.79	51.51	62.64	89.77	112.24	144.78	171.73	200.89
Region II (b)											
PE3 distribution											
***P* %**	1	5	10	20	25	50	80	90	96	98	99
T_{year}	1.01	1.05	1.11	1.25	1.33	2	5	10	25	50	100
***Q* (*F*)**	176.03	177.05	178.92	184.07	187.28	210.65	272.13	321.93	389.83	442.16	495.06
GPA distribution											
***P* %**	1	5	10	20	25	50	80	90	96	98	99
T_{year}	1.01	1.05	1.11	1.25	1.33	2	5	10	25	50	100
***Q* (*F*)**	173.08	175.32	178.29	184.81	188.43	211.82	269.23	317.79	389.23	441.55	494.99
Region III (c)											
GPA distribution											
***P* %**	1	5	10	20	25	50	80	90	96	98	99
T_{year}	1.01	1.05	1.11	1.25	1.33	2	5	10	25	50	100
***Q* (*F*)**	26.11	27.16	28.10	29.80	30.67	36.13	50.83	65.14	89.23	112.03	139.37
GNO distribution											
***P* %**	1	5	10	20	25	50	80	90	96	98	99
T_{year}	1.01	1.05	1.11	1.25	1.33	2	5	10	25	50	100
***Q* (*F*)**	26.91	27.42	28.09	29.58	30.42	36.05	51.23	65.45	88.79	110.65	136.96

In the estimates of $Q_{(1.11,\ 1.25,\ 1.33)}$, which are the main body of the distribution, AMS, PDS-I, and PDS-III are listed from largest to smallest. From Q_2 to Q_{100}, AMS, PDS-I, and PDS-III had very high estimates. PDS-II flood discharges were estimated almost the same from $Q_{1.01}$ to $Q_{1.33}$, and increased rapidly from the main body of the distribution to the upper tail. From Q_{10} to Q_{100}, AMS and PDS-II produced similar predictions.

The values obtained as a result of regional analyses vary. However, as an alternative to annual maximum floods, the PDS-I and PDS-III data sets in the lower tail of the distribution can be used. The PDS-II data set can be used in the upper tail of the distribution (Karim et al. 2017, Zadeh et al. 2019, Ahmad et al. 2019). Since the partial duration, flood estimations are lower than annual maximum estimations, they can provide advantages for engineering projects at lower costs (Pan et al. 2022). For the main body of the distribution, the PDS-II data set is not recommended in terms of cost since it gives higher estimates than the AMS data set, except for $Q_{(25,50,100)}$ (Figure 6).

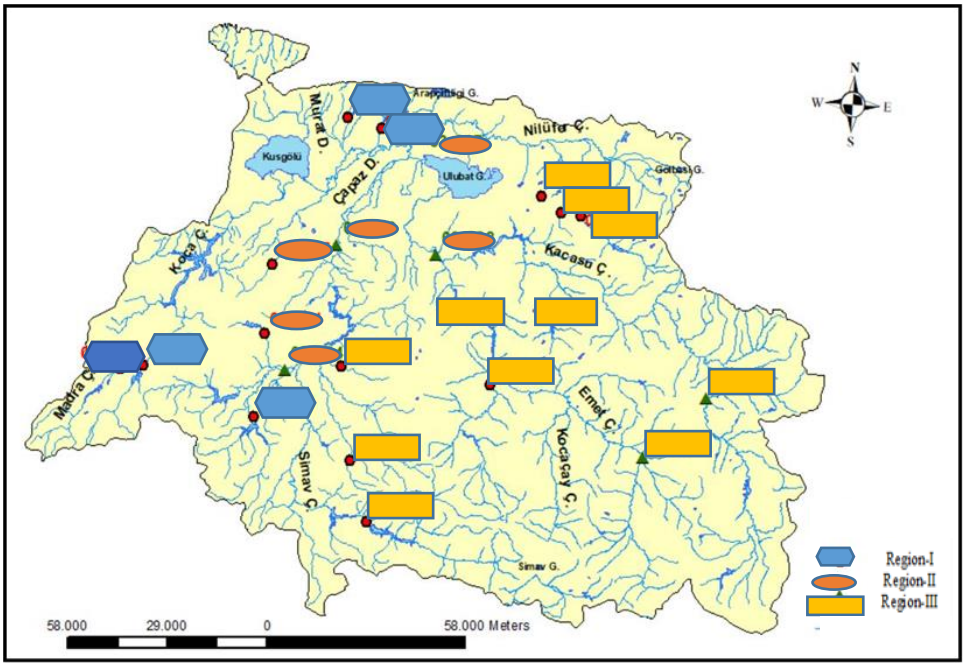

Figure 5- Location of stations in homogeneous regions obtained according to partial duration flood series

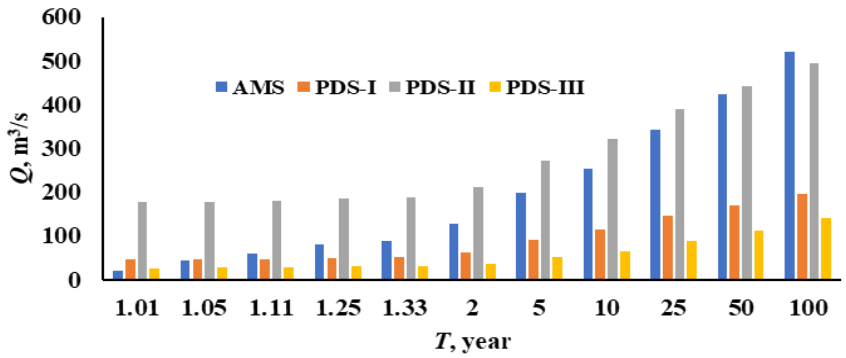

Figure 6- Comparison of the regional design flood discharges of annual maximum and partial duration flood series
***AMS: Annual maximum series, PDS-I: Partial duration series for Region I, PDS-II: Partial duration series for Region II, PDS-III: Partial duration series for Region III**

In our study, we performed regionalization of flood frequency analysis and used L-moments as the parameter estimation method. L-moments have a significant advantage over other ordinary product moments because they are calculated by linear combinations of data without squaring and cubing them. It is unbiased in its predictions of quantiles in the lower and upper tails of the distribution and provides strong estimates of the probability distribution parameters. On the other hand, it makes unbiased predictions by using L-moment ratios to measure the discordancy, heterogeneity, and goodness of fit tests. Finally, it produces highly advantageous results over at-site estimates through the regional L-moment algorithm (Anlı 2009, Zadeh et al. 2019). According to the regional homogeneity results, the design of flood discharges for both data sets obtained in various return periods according to the purpose in terms of the flood risk of the basin can be used in practice, as mentioned above. The flood discharges can be used appropriately in city drainage networks and infrastructure projects from the design of the elements of the water storage (hydraulic) structures (Durocher et al. 2019). However, it's important to note that there are a large number of flow observation stations (more than 80) in the basin, but only 22 of them could be selected because they have sufficient observation periods and regular streamflow data. Some of the remaining stations have been closed, and some have become unable to perform their duties due to urbanization. Therefore, only 22 stations that were not intervened could be selected.

3.3. At-site flood frequency analysis

The at-site frequency analysis was a crucial part of our study, as it was performed for flood data sets at all stations for annual maximum and partial duration series. The analysis revealed that the partial duration flood series fits all distributions. In contrast, the data from D03A013 and D03A085 stations do not fit the logarithmic gamma distribution for the annual maximum flood series. The most appropriate frequency distributions and relevant Kolmogorov-Smirnov test values for annual maximum and

partial duration flood series are shown in Table 13. According to Table 13, GPA was the most dominant distribution for both data sets among the at-site frequency distributions. This situation has also been seen in partial-duration flood series with very high suitability and other distributions adapted to less data and in the annual maximum flood series, GLO, FRE3, LP3, and LLO3 distributions provided the best fit to the data, while other distributions adapted to less data. Using the most appropriate distributions for both data sets, the at-site design flood discharges for certain return periods were obtained with the L-moment parameter estimation method and are given for comparison in Figure 7. According to the at-site frequency analysis results, in the lower tail of the distribution (short-term return periods), at D03A008, D03A013, D03A024, D03A044, D03A051, D03A052, D03A056, D03A064, D03A082, D03A084, D03A086, D03A087, D03A096, and E03A028 stations, both data sets produced estimates of design flood discharges close to each other. In the main body of the distribution (medium-term return periods), design flood discharges of both data sets produced close estimates to each other at stations D03A013, D03A024, D03A044, D03A056, E03A002, E03A011, E03A016, E03A024, E03A028 and E03A031. In the upper tail of the distribution (long-term return periods), design flood discharge estimates of both data sets were close to each other at stations D03A086, E03A002, E03A011, E03A016, E03A017, and E03A031. The stations whose estimations are close to each other in both short-term and medium-term return periods are D03A013, D03A024, D03A044, D03A056, E03A024, and E03A028. The stations whose estimations are close to each other in both medium-term and long-term return periods are E03A011, E03A016, and E03A031. Station data whose forecasts for all three periods were close to each other could not be determined. As can be understood from the expressions, using partial duration flood series as an alternative to annual maximum flood series in at-site frequency analysis is more appropriate, especially for the short and medium term. In long-term estimations, partial duration series at fewer stations can be an alternative to the annual maximum flood series (Kiran and Srinivas 2021).

Table 13- The best-fit frequency distributions and relevant Kolmogorov-Smirnov test values for both data series

		Annual Maximum Series		*Partial Duration Series*	
N	***Station Code***	***K-S***	***Best-fit Frequency Distribution***	***K-S***	***Best-fit Frequency Distribution***
1	D03A008	0.093	GG4	0.054	GPA
2	D03A013	0.107	LP3	0.079	FRE3
3	D03A024	0.065	LP3	0.067	GPA
4	D03A034	0.062	WE3	0.069	GPA
5	D03A044	0.070	LP3	0.285	LN3
6	D03A051	0.128	LLO3	0.063	GPA
7	D03A052	0.077	LN	0.055	GPA
8	D03A056	0.079	FRE3	0.090	G3
9	D03A064	0.073	FRE3	0.606	WE3
10	D03A082	0.109	LLO3	0.088	GPA
11	D03A084	0.070	GPA	0.059	FRE3
12	D03A085	0.110	WE	0.100	GPA
13	D03A086	0.073	GG4	0.062	LN
14	D03A087	0.081	G3	0.075	GPA
15	D03A096	0.093	GLO	0.053	GPA
16	E03A002	0.106	WE	0.063	G3
17	E03A011	0.101	GLO	0.069	GPA
18	E03A016	0.806	LLO3	0.058	GG4
19	E03A017	0.061	GLO	0.083	GPA
20	E03A024	0.086	G	0.081	LLO3
21	E03A028	0.085	FRE3	0.068	GG4
22	E03A031	0.142	GLO	0.051	FRE3

*K-S: Kolmogorov-Smirnov test value, EXP: Exponential, EXP2: 2-parameter exponential, FRE: Frechet, FRE3: 3-parameter Frechet, G: Gamma, G3: 3-parameter gamma, GEVs: Generalized extreme values, GG: Generalized gamma, GG4: 4-parameter generalized gamma, GLO: Generalized logistic, GPA: Generalized Pareto, LLO: Logarithmic logistic, LLO3: 3-parameter logarithmic logistic, LP3: 3-parameter logarithmic Pearson, LO: Logistic, LN: Logarithmic normal, LN3: 3-parameter logarithmic normal, N: Normal, WE: Weibull, WE3: 3-parameter Weibull.

Figure 7- Comparison of the at-site design flood discharges at certain return periods for both series

4. Conclusions

This study investigated the possibilities of using partial duration flood series as an alternative to annual instantaneous maximum flood series on an at-site and regional basis using the regional index-flood approach in the Susurluk river basin. The annual maximum flood series provided homogeneity in the Susurluk basin as a single region, and regionally designed flood discharges were estimated for hydraulic structures and flood offset in short, medium- and long-term return periods according to the one suitable GLO distribution. According to annual maximum flood data, since the basin is homogeneous, it has been revealed that design flood discharges can be considered for the entire Susurluk basin. The variance-mean ratio method was used while selecting partial duration flood series, and various frequency factors were used to extract peaks over the threshold. The most appropriate frequency factors for the data sets were determined according to the Poisson distribution, which makes the variance-mean ratio equal. k=3.5 was determined for only two stations. k=4 was suitable for seven stations, and k=5 was suitable for thirteen stations. For the k=5 value chosen at station E03A017, the total m (number of partial duration flood) value was smaller than the n (number of annual maximum flood) ($m < n$), so a frequency factor of k=4.5 was considered. The average number of peaks over the threshold level (λ`) varies between 1.26 and 5.31. The lowest flood data ($\lambda$`=1.26, m=48) was extracted at station E03A017, and the highest (λ`=5.31, m=154) was extracted at station D03A085. The basin was divided into three sub-regions by cluster analysis according to partial duration series. After ensuring homogeneity in three separate regions, regionally designed flood discharges were estimated for hydraulic structures and flood offset in short- medium- and long-term return periods according to PE3 and GPA distributions. In a regional comparison of data sets, it can be considered that PDS-I and PDS-III data sets can be used as an alternative to annual maximum floods for the lower tail of the distribution, and PDS-II data sets can be used for the upper tail of the distribution. The PDS-II data set for the main body of the distribution, except for the upper tail of the distribution, is not recommended from a cost perspective as it gives higher estimates than the AMS data set. In at-site frequency analysis, using partial duration flood series as an alternative to annual maximum flood series is more appropriate, especially in the short and medium term. In long-term estimations, a partial duration series at fewer stations can be an alternative to the annual maximum flood series. The study concluded that partial duration flood series can be used in many stations in the short and medium term instead of annual maximum flood series but can be used in fewer stations in the long term. Since partial duration flood estimations are lower than annual maximum ones, they can provide advantages to engineering projects with lower costs (Yue et al. 2022).

At the end of the study, some important points where partial duration series are advantageous in flood frequency analysis are listed below:

- Due to the extracting process (peaks-over-threshold), the partial duration series is not limited to smaller sample sizes than the annual maximum series, as the overall data length is flexible.
- Due to the width of the data set, partial duration series are effective in estimating frequent floods needed by the ecosystem.
- Partial duration series can be useful in regionalizing floods, which are common due to data extraction.
- Due to the controllability of the time series, partial duration series are more suitable for performing non-stationary flood frequency analysis.

Acknowledgments

This study was produced from the MSc thesis of Ayşe Doğanülker under the supervision of Alper Serdar Anli.

References

Adamowski K (2000). Regional analysis of annual maximum and partial duration flood data by nonparametric and L-moment methods. *Journal of Hydrology* 229(3): 219-231 doi:10.1016/s0022-1694(00)00156-6

Adamowski K, Liang G & Patry G G (1998). Annual maxima and partial duration flood series analysis by parametric and non-parametric methods. Hydrological Processes 12: 1685-99

Agilan V, Umamahesh N V & Mujumdar P P (2020). Influence of threshold selection in modeling peaks over threshold-based nonstationary extreme rainfall series. *Journal of Hydrology* 593: 125625

Ahmad I, Laksacia A, Chikr-Elmezouar Z, Almanjahie Ibrahim M & Khan DA (2019). At-site rainfall frequency analysis of partial duration series and annual maximum series using L-moments in Rawalpindi city of Pakistan. Applied Ecology and Environmental Research 17(4): 8351-8367. http://dx.doi.org/10.15666/aeer/1704_83518367.

Amorim R & Villarini G (2024). Assessing the performance of parametric and non-parametric tests for trend detection in partial duration time series. *Journal of Flood Risk Management* 17(1): e12957

Anlı A S (2009). Regional frequency analysis of rainfall data in Ankara province using L-moment methods. Ankara University, PhD thesis (In Turkish).

Anli A S, Apaydin H & Ozturk F (2007). Regional flood frequency estimation for the Göksu river basin through L-moments. In International River Basin Management Conference, State Hydraulic Works (pp. 22-24).

Ashkar F & Ba I (2017) Selection between the generalized Pareto and kappa distributions in peaks-over-threshold hydrological frequency modelling. *Hydrological Sciences Journal* 62(7): 1167–1180.

Basu B & Srinivas V V (2016). Evaluation of the index-flood approach related regional frequency analysis procedures. *Journal of Hydrologic Engineering* 21(1): 04015052. https://doi.org/10.1061/(asce)he.1943-5584.0001264

Ben-Zvi A (1991). Observed advantage for negative binomial over Poisson distribution in partial duration series. Stochastic Hydrology and Hydraulics 5(2): 135–146

Bezak N, Brilly M & Šraj M (2014). Comparison between the peaks-over-threshold method and the annual maximum method for flood frequency analysis. *Hydrological Sciences Journal* 59(5): 959–977

Cunnane C (1979). A note on the Poisson assumption in partial duration series models. Water Resources Research 15: 489-94

Dalrymple T (1960). Flood frequency analyses. Water Supply Paper 1543-A, U.S. Geological Survey, Reston, Va.

Doğanülker A (2022). Flood Frequency Analysis in Susurluk River Basin. Ankara University, MSc. thesis (In Turkish).

Durocher M, Burn D H & Ashkar F (2019). Comparison of estimation methods for a nonstationary index-flood model in flood frequency analysis using peaks over threshold. Water Resources Research 55(11): 9398–9416

Fill H D & Steiner A A (2003). Estimating instantaneous peak flow from mean daily flow data. *Journal of Hydrologic Engineering*, Vol. 8, No. 6, November 1, 203: 365-369

Greenwood J A, Landwehr J M & Matalas N C (1979). Probability weighted moments: Definition and relation of parameters of several distributions expressible in inverse form. Water Resources Research 15: 1049-1054

Guru N (2016). Flood frequency analysis of partial duration series using soft computing techniques for Mahanadi River basin in India. National Institute of Technology Rourkela-769008. Doctor of Philosophy

Guru N (2022). Implication of partial duration series on regional flood frequency analysis, *International Journal of River Basin Management*, 22:2, 167-186, DOI: 10.1080/15715124.2022.2114486.

Gürler Ç, Anli AS & Polat H E (2024). Developing regional hydrological drought risk models through ordinary and principal component regression using low-flow indexes in Susurluk basin, Turkey. Water 16, no. 11: 1473. https://doi.org/10.3390/w16111473.

Haktanır T (1991). Practical computation of gamma frequency factors. Hydrological Sciences 36,6: 559-610.

Haktanır T & Bozduman A (1995). A study on sensitivity of the probability weighted method on the choice of the plotting position formula. *Journal of Hydrology* 168: 265-281

Hosking J R (1986). Estimation of the generalized extreme value distribution by the method of probability-weighted moments. Technometrics 27: 251-261

Hosking J R M (1990). L-moments: Analysis and estimation of distributions using linear combinations of order statistics. *Journal of the Royal Statistical Society*. Series B 52(1): 105-124

Hosking J R M & Wallis J R (1993). Some statistics useful in regional flood frequency analysis. Water Resources Research 23: 271-281.

Hosking J R M & Wallis J R (1997). Regional frequency analysis an approach based on L-moments, Cambridge University Press.

Hosking J R M (2005). Fortran routines for use with the method of L-moments, Version 3.04. Research Report RC 20525, IBM Research Division, T.C. Watson Research Center, Yorktown Heights, N.Y.

Karim F, Masud H & Marvanek S (2017). Evaluating annual maximum and partial duration series for estimating frequency of small magnitude floods, Water 9, no. 7: 481. https://doi.org/10.3390/w9070481.

Kiran K G & Srinivas VV (2021). Distributional regression forests approach to regional frequency analysis with partial duration series. Water Resources Research, 57, e2021WR029909. https://doi.org/10.1029/2021WR029909.

Kjeldsen T R, Smithers J C & Schulze R E (2002). Regional flood frequency analysis in the KwaZulu-Natal province, South Africa, using the index-flood method. *Journal of Hydrology* 255: 194-211

Lang M, Ouarda T B M J & Bobée B (1999). Towards operational guidelines for over-threshold modeling, *Journal of Hydrology* 225(3-4): 103- 117

Madsen H, Rasmussen P F & Rosbjerg D (1997a). Comparison of annual maximum series and partial duration series methods for modeling extreme hydrologic events. 1. At-site modeling. Water Resources Research, 33: 747-57

Madsen H, Pearson C P & Rosbjerg D (1997b). Comparison of annual maximum series and partial duration series methods for modeling extreme hydrologic events. 2. Regional modeling. Water Resources Research 33: 759-769

Öney M & Anlı A (2023). Regional drought analysis with standardized precipitation evapotranspiration index (SPEI): Gediz basin, Turkey. *Journal of Agricultural Sciences* 29(4): 1032-1049. https://doi.org/10.15832/ankutbd.1030782.

Önöz B (1994). A new parameter estimation method, probability weighted moment method. DSI Technical Bulletin, 81: 49-54 (In Turkish).

Pan X & Rahman A (2021). Comparison of annual maximum and peaks-over-threshold methods with automated threshold selection in flood frequency analysis: a case study for Australia. Natural Haz. https://doi.org/10.1007/s11069-021-05092-y.

Pan X, Rahman A, Haddad K & Ouarda T B (2022). Peaks-over-threshold model in flood frequency analysis: a scoping review. Stochastic Environmental Research and Risk Assessment 36(9): 2419-2435

Pham H X, Shamseldin A Y & Melville B (2014). Statistical properties of partial duration series: Case study of North Island, New Zealand. *Journal of Hydrologic Engineering* 19(4): 807-815

Rahman A S, Rahman A, Zaman M A, Haddad K, Ahsan A & Imteaz M (2013). A study on selection of probability distributions for at-site flood frequency analysis in Australia. Natural Hazards 69(3): 1803-1813

Rasmussen P F & Rosbjerg D (1991). Prediction uncertainty in seasonal partial duration series. Water Resources Research 27: 2875-83.

Rosbjerg D & Madsen H (1992). On the choice of threshold level in partial duration series, Proc. Nordic Hydrological Conference, Alta (ed. G. Østrem), NHP Rep. no. 30: 604-615

Rosbjerg D, Madsen H & Rasmussen P F (1992). Prediction in partial duration series with generalized Pareto-distributed exceedances. Water Resources Research 28: 3001-3010

Seçkin N (2009). Regional flood frequency analysis with index-flood method based on L-moments, Çukurova University, PhD. Thesis, Adana.

Seckin N & Topcu E (2016). Regional frequency analysis of annual peak rainfall of adana and the vicinity. Journal of the Faculty of Engineering and Architecture of Gazi University 31(4): 1049-1062

Stedinger J R (1983). Estimating a regional flood frequency distribution. Water Resources Research 19(2): 503-510

Sveinsson O G B, Salas J D & Boes D C (2003). Uncertainty of quantile estimators using the population index flood method. Water Resources Research, 39(8): 1206. https://doi.org/10.1029/2002wr001594.

Swetapadma S & Ojha C (2021). Technical Note: Flood frequency study using partial duration series coupled with entropy principle. Hydrology and Earth System Sciences. https://doi.org/10.5194/hess-2021-570

SYGM (2022). Susurluk basin flood management planning report, General Directorate of Water Management, Ankara (In Turkish).

Topcu E & Seckin N (2016). Drought analysis of the Seyhan Basin by using standardized precipitation index SPI and L-moments. *Journal of Agricultural Sciences* 22(2): 196-215

Van Campenhout J, Houbrechts G, Peeters A & Petit F (2020). Return period of characteristic discharges from the comparison between partial duration and annual series: Application to the Walloon Rivers (Belgium). Water 12: 792. https://doi.org/10.3390/w12030792.

Wilks D S (1993). Comparison of three-parameter probability distributions for representing annual extreme and partial duration precipitation series. Water Resources Research 29: 3543-49.

Yue Z, Xiong L, Zha X, Liu C, Chen J & Liu D (2022). Impact of thresholds on nonstationary frequency analyses of peak over threshold extreme rainfall series in Pearl River Basin, China. Atmospheric Research 276: 106269

Zadeh S, Durocher M, Burn & Ashkar F (2019). Pooled flood frequency analysis: a comparison based on peaks-over threshold and annual maximum series, *Hydrological Sciences Journal* 64(2): 121-136, DOI:10.1080/02626667.2019.1577556.